# Design and Simulation of Nano-Plasmonic Biosensors

By Sina Pourjabar

B.S. in Electrical Engineering February 2013, University of Tabriz

A Thesis submitted to

The Faculty of
School of Engineering and Applied Sciences
of The George Washington University
in partial fulfillment of the requirements
for the degree of Master of Science

May 15th, 2016

Thesis directed by

Mona E. Zaghloul
Professor of Engineering and Applied Science

# Dedication

To my beloved family for their endless love, unfailing devotion and enduring support

# Acknowledgments

First, I would like to express my deepest appreciation to my adviser professor Mona Zaghloul for her feedback and constant support throughout my thesis research. I gained a great amount of experience under her supervision.

I would also like to thank Dr. Zhenyu Li who opened my eyes to the application of electronics in the biomedical field during my first semester in GW which created the first spark in me to choose my master's thesis in the field of biosensors.

I would like to thank professor Shahrokh Ahmadi for motivating the ECE students throughout their enduring path; he truly he deserved the 2016 Distinguished Teacher Award in the ECE department.

I would like to expand my gratitude to professor Can Korman, Dr. Jerry Wu and Dr. Tony Ivanov who were supportive of me as a graduate student and helped me to create a strong background in the field of VLSI and microelectronics.

I would like to thank Mark Aglipay for being responsive and helping me so many times when there was a technical issue in the laboratory and the simulation software.

Finally, I am grateful for my family who are always there for me and my friends for refreshing my spirit.

# Abstract of Thesis

## Design and Simulation of Nano-Plasmonic Biosensors

Detection of biomolecules in low concentration specimens has a long way to achieve a high precision, low cost and be accessible as a portable device. One proposed method that has the advantage of label free detection of biomolecules is by use of nano plasmonic sensors. Nano plasmonic biosensor is composed of metallic nanoparticle on a dielectric material. In a certain wavelength of the incident light these metallic sensors create a strong localized electric field that is extremely sensitive to an adjacent material, creating a highly sensitive sensor. Producing a higher electric field results in a more sensitive sensor for detection.

To our knowledge, there is no study which mentions the appropriate size of the nanoparticles that can produce the highest amount of electric field. In this thesis, Lumerical FDTD software was used to model and compare three different types of nano plasmonic sensors in terms of the created electric field. In addition, a bow tie structure with the optimum size was studied and was able to produce an enhanced field of 90 times of the incident electric field. This, results in an improved sensitivity.

Finally, the sensitivity of the bow tie sensor in the proximity of a simulated dielectric with the diameter of 20 nm was examined. The sensor was able to make a 10.5 nm shift in the peak resonance wavelength. The result of this thesis revealed that creating a sensor with a sharp edge generates a more enhanced field with a narrower linewidth in the resonance spectrum.

# Table of Contents

**Dedication** ..... **ii**

**Acknowledgments** ..... **iii**

**Abstract of Thesis** ..... **iv**

**Table of Contents** ..... **v**

**List of Figures** ..... **viii**

**List of Symbols/Nomenclature** ..... **x**

**Chapter 1: Introduction** ..... **1**

1.1 Background ..... 1

1.2 Problems to Be Solved ..... 2

1.3 Organization of the Thesis ..... 2

**Chapter 2: Theoretical Background** ..... **4**

2.1 Background ..... 4

2.2 LSPR ..... 7

2.3 Mie Theory ..... 9

**Chapter 3: Plasmonic Sensors in the Literature** ..... **12**

3.1 Plasmonic in Sensing ..... 12

3.2 Enhancing the Resonance Shift .....16

3.3 Molecular Tuning.....17

3.4 Raman Scattering .....17

**Chapter 4: Simulation and Results .....19**

4.1 Simulation .....19

4.2 Nanotriangle Array .....20

4.3 Nanoantenna.....22

4.3.1 Sweeping Length.....25

4.3.2 Sweeping Width.....25

4.3.3 Sweeping Thickness.....27

4.4 Bow tie .....29

4.5 Dielectric.....33

**Chapter 5: Applications.....36**

5.1 Gas Sensor.....36

5.2 PH Sensor.....37

5.3 Multiplexing.....37

5.4 Microfluidic Chip.....38

5.5 Imaging and Treatment ..... 38

5.6 Solar cells ..... 39

**Chapter 6: Conclusion ..... 41**

**References ..... 43**

**Appendix ..... 48**

# List of Figures

Figure Page

2.1 Demonstration of localized surface plasmons .....7

2.2 Real and imaginary parts of the dielectric function of the gold.....8

3.1 Definition of linewidth and shift in the peak resonance .....13

3.2 Nanospherical polymers before metal deposition.....13

3.3 Silver nanotriangles with the circular structure .....14

3.4 Red shift in the resonance peak for chemicals with different refractive index.....15

4.1 Simulation interface for gold nanotriangle using FDTD .....21

4.2 Extinction cross section .....21

4.3 Electric filed enhancement at the resonance frequency.....22

4.4. Simulation of nanoantena .....23

4.5. nanoantenna distance sweep .....23

4.6. Impact of distance on electric field coupling.....24

4.7 Single nanobar filed enhancement.....24

4.8 Increasing the nanoantenna's length.....25

4.9 Increasing the nanoantenna's Width.....26

4.10 Effect of width in the field enhancement.....26

4.11 Effect of thickness in the resonance peak .....27

4.12 Thickness effect in the electric field .....27

4.13 Relation between scattering and absorption cross section .....28

4.14 Bow tie perspective view .....29

4.15 Relation between base and the resonance peak .....29

4.16 Decreasing base size from 50 nm to 30 nm creates higher electric filed.....30

4.17 Bow tie distance sweep .....31

4.18 Effect of distance on enhancing electric field in the bow tie structure .....32

4.19 Water nanosphere in the middle of bow tie structure .....33

4.20 Red shift after placing water .....34

4.21 Water nanosphere in the middle of nanoantenna .....34

5.1 Hydrogen gas detection.....36

5.2 Multiplexing in detection .....37

5.3Microfluidic Chip.....39

5.4 Metallic nanoparticles in solar cells .....40

# List of Symbols/Nomenclature

$\varepsilon_0$ : Permittivity of free space

$\varepsilon(\omega)$ : Dielectric function of a medium as a function of frequency

$m^*$ : Effective mass of electron

m: Bulk refractive index sensitivity

$\Gamma$ : Linewidth of the peak resonance

E(t): Electric field as a function of time

x(t): Displacement as a function of time

$\omega_p$ : Plasma frequency of free electron gas

P: Dipole moment inside

D: Electric displacement field

n: Number of electrons

s: Sensitivity

e: Electron charge

$\lambda_p$ : Peak resonance wavelength

$n_{medium}$ : Refractive index of the medium

$p_{scat}$ : Scattering power

$p_{abs}$ : Absorbed power

I: Incident wave intensity

$\alpha$ : Polarizability

$\sigma$ : Scattering or absorption cross section

$\gamma$ : Damping frequency of plasma

Q: Efficiency factor

# Chapter1: Introduction

## 1.1 Background

Before the invention of transistors in 1974, vacuum tubes were used to build computers, radios and televisions. Being extremely power hungry and big in dimensions for vacuum tubes, resulted in the huge sized and expensive computers that nobody except companies could afford. Passing through the decades with the invention of transistors and the ability to fabricate millions of transistors in dimensions smaller than a dime, not only the size and price of the computers dropped but the new generation of the computers experimented a huge boost in the processing speed. As a result, having a small computer for each person that once were impossible to buy became possible. Similar to the big old computers the problem still exists in the biomedical field.

Nowadays, big and expensive medical laboratories have the responsibility of taking blood or urine samples from patients and perform a time consuming analysis in order to tell them whether they have any sort of diseases or not. In addition, some diseases such as cancer are better to be detected at the early stages of development so that better approaches could be prescribed. However, these tests might be costly and may not be affordable to everyone. This is one of the reasons that nano-plasmonic sensors are becoming famous. It would be a great contribution to the humanity to be able to make an affordable and a simple device that helps to keep track of the health of a person and one's quality of life.

## 1.2 Problems to Be Solved

Previously investigated nano-plasmonic sensors by researchers, although look promising for detection, still have the problem of low sensitivity[1].

The purpose of this work is to further increase the sensitivity of the nano-plasmonic sensors through finding the right structure with the optimum dimensions that leads to the highest amount of created electric field. Before going into details first some characteristics of metals are explained.

## 1.3 Organization of the Thesis

This thesis consists of 6 chapters:

Chapter 1 gives a brief background about the biomedical detection, the reason that nano-plasmonic sensors are becoming important and the problems that need to be solved in these sensors.

Chapter 2 discuses about the theoretical background of the interaction between electromagnetic waves and metallic nanoparticles that create plasmon.

Chapter 3 describes previous studies of researchers on the field of nano-plasmonic and possible ways to enhance the sensitivity of these sensors.

Chapter 4 gives a brief explanation of the simulation software used in this thesis and focuses on comparing different sensor structures and size optimization of the sensor for the best sensitivity.

Chapter 5 introduces application of nano-plasmonic sensors in other areas of study such as gas sensors, thermal imaging and solar cells.

Chapter 6 is the conclusion chapter which gives a summary of the results and works that has been done in the simulation.

# Chapter 2: Theoretical Background

In this chapter the theory of the interaction between electromagnetic waves and metallic nanoparticles which leads to the plasmons has been described.

## 2.1 Background

One property of metals is that the electromagnetic waves cannot penetrate through them. This is the reason that metals are shiny in visible spectrum of light. However, as the frequency of the electromagnetic waves increases close to ultraviolet, they can propagate through the metal. At optical frequencies, dielectric functions of metals play an important role in defining the specifications of the metals.

Permittivity of metals is a function of frequency and can be described as:

$$\varepsilon(\omega) = \varepsilon 1(\omega)+i\varepsilon 2(\omega) \quad (2.1)$$

The real part of the $\varepsilon(\omega)$ shows the absorption while the imaginary part responds to dissipation of EM wave in metals [2].

In a metal, electrons in the conduction band can move freely inside the metal. Plasma oscillation is the collective oscillation of free electrons. A quantization of these collective oscillation of electrons is called plasmon [3],[4].

As mentioned above, collective oscillation of free electron is called plasmon [3],[4]. Equation (1.2) shows the relation between the displacement field and an applied electric field to a medium. P is a created dipole moment inside a medium, it is also called polarization density.

$$D(\omega) = \varepsilon_0 \varepsilon(\omega) E(\omega) = \varepsilon_0 E(\omega) + P(\omega) \tag{2.2}$$

In Drude-Sommerfield model, motion equation for the free electron gas exposed to an external electric field is written as:

$$m^* \frac{\partial^2 x}{\partial t^2} + m^* \gamma \frac{\partial x}{\partial t} = -eE(t) \tag{2.3}$$

In which "$m^*$" is effective mass of electron and gamma is described as the damping frequency of free electrons which is a result of collision among electrons and is usually 100 THz [3].

$$\gamma = 1/\tau \tag{2.4}$$

With the assumption of harmonic electric field with the respect to time:

$$E(t) = E_0 e^{-i\omega t} \tag{2.5}$$

Solving the equation gives:

$$x(t) = \frac{e}{m^*(\omega^2 + i\gamma\omega)} E(t) \tag{2.6}$$

$$P = -nex \tag{2.7}$$

$$\rightarrow P = -\frac{ne^2}{m(\omega^2 + i\gamma\omega)} E \tag{2.8}$$

Placing in equation (2.2) $D = \varepsilon_0 (1 - \frac{\omega_p^2}{\omega^2 + i\gamma\omega}) E$ (2.9)

Thus, dielectric function of the free electron gas can be written as:

$$\varepsilon = (1 - \frac{\omega_p^2}{\omega^2 + i\gamma\omega}) \tag{2.10}$$

At optical frequencies free electrons in metals act as a plasma with the oscillation frequency of [3]:

$$\omega_p = \sqrt{\frac{ne^2}{m^* \varepsilon_0}} \tag{2.11}$$

In which:

n: Density of electrons.

$m^*$ : Effective mass of electron.

e: Electric charge of an electron.

$\varepsilon_0$ : Permittivity of the free space.

Equation (2.10) can be written as $\varepsilon(\omega) = \varepsilon_1(\omega) + i\varepsilon_2(\omega)$ with the real and imaginary part of:

$$\varepsilon_1(\omega) = 1 - \frac{\omega_p^2 \tau^2}{1 + \omega^2 \tau^2} \tag{2.12}$$

$$\varepsilon_2(\omega) = \frac{\omega_p^2 \tau}{\omega(1 + \omega^2 \tau^2)} \tag{2.13}$$

By increasing the frequency of the EM wave metals lose their ability to reflect these waves, instead we have absorption in the metal. In addition, at a certain frequency metals show highest amount of absorption which is called resonance frequency. Resonance

frequency for noble metals such as gold and silver lies in the visible frequency of light spectrum[3].

## 2.2 LSPR

Localized surface plasmon resonance (LSPR) are the localize oscillation of electrons in a metallic nanoparitcle. When light shines on a metallic nanoparticle with dimensions smaller than wavelength of the light (d<<lambda), because of the subwavelength size of nanoparticle we can assume that the applied EM wave is constant over the nanoparticle. This would lead to a dipole moment P. The calculated dipole moment is for a sphere with a radius of "a" is expressed as [3]:

$$P = 4\pi\varepsilon_0\varepsilon_m a^3 \frac{\varepsilon - \varepsilon_m}{\varepsilon + 2\varepsilon_m} E_0 \tag{2.14}$$

It can also be written as $P = \varepsilon_0\varepsilon_m \alpha E_0$ (2.15)

In which $\alpha$ is called polarizability : $\alpha = 4\pi a 3 \frac{\varepsilon - \varepsilon_m}{\varepsilon + 2\varepsilon_m}$ (2.16)

At $real[\varepsilon] = -2\varepsilon_m$, alpha and as result P reach to their maximum values.

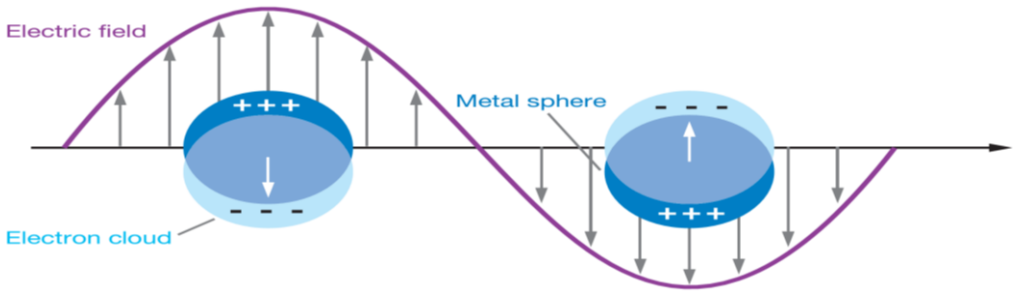


**Figure 2.1 Demonstration of localized surface plasmons [5]**

Therefore, any material with a negative dielectric function can have a dipole moment that leads to the plasma oscillation of electrons. Noble metals such as gold and silver have a complex dielectric function with a negative real and a small imaginary part. Figure 1.2 shows the dielectric function of the gold in the visible spectrum of light [6].

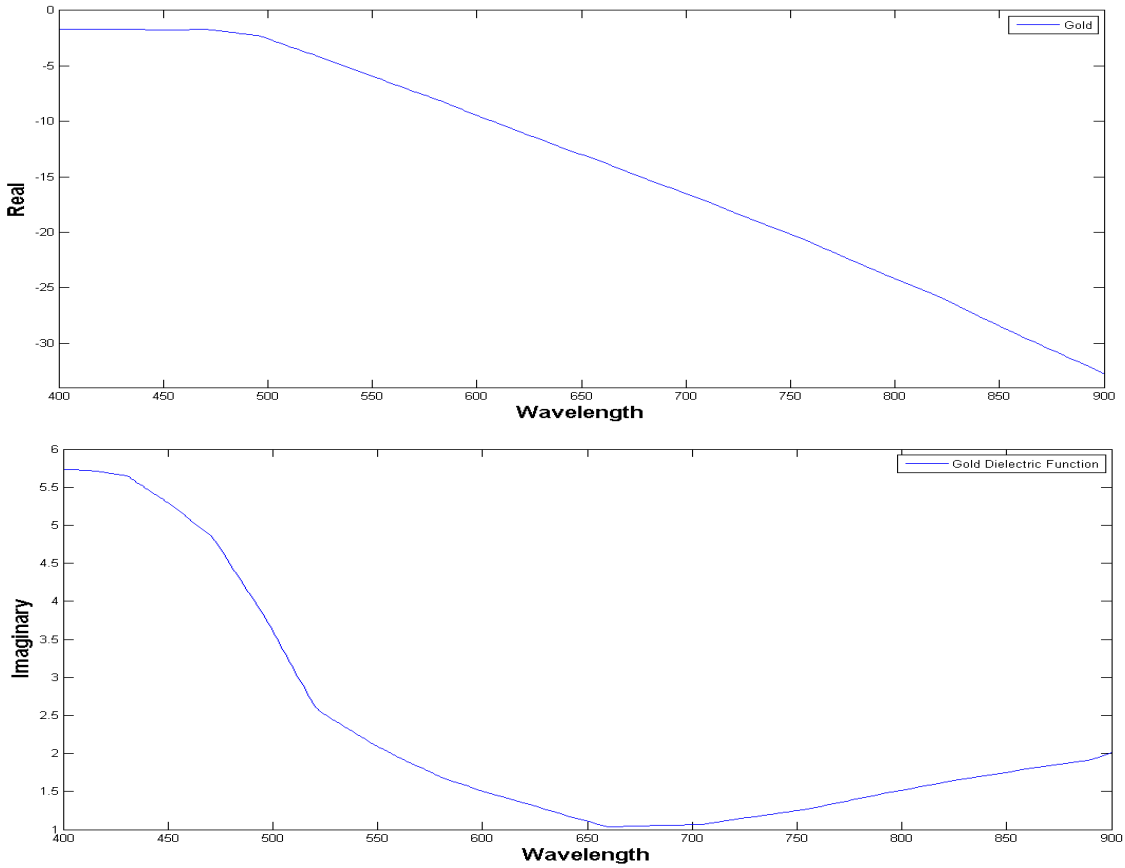


**Figure 2.2 Real and imaginary parts of the dielectric function of the gold [6]**

## 1.3 Relation between refractive index and peak wavelength

As mentioned in equation (2.4) $\gamma = 1/\tau$ . Therefore, $\varepsilon_1(\omega)$ for a metal could also be written as [4]:

$$\varepsilon_1(\omega) = 1 - \frac{\omega_p^2}{\omega^2 + \gamma^2} \tag{2.17}$$

For visible and near infrared frequencies $\gamma << \omega_p$ [3], so $\varepsilon_1(\omega) = 1 - \frac{\omega_p^2}{\omega^2}$ (2.18)

We know that the resonance occurs at the condition $\varepsilon_1 = -2\varepsilon_m$ . By putting this statement in equation (2.18) we achieve to the peak frequency of resonance:

$$\omega_{\max} = \frac{\omega_p}{\sqrt{2\varepsilon_m + 1}} \tag{2.19}$$

In addition $\lambda = \frac{2\pi c}{\omega}$ and $\varepsilon = n^2$ so equation (2.19) could be re written as [4]:

$$\lambda_m = \lambda_p \sqrt{2n_m^2 + 1} \tag{2.20}$$

## 2.3 Mie Theory

Mie theory, established by Gustav Mie, presents an analytical solution to Maxwell equation for metallic nanoshperes. The equation describes the absorption and scattering in metallic spherical particles which could explain the different colors of gold nanospheres in optical frequencies [7].

When a nanoparticle is exposed to light, absorption and scattering of the light occurs. In other words, absorption and scattering are removed energy from light as a result of hitting a subwavelength nanoparticle. It is also worth mentioning that scattering and absorption are responsible for the color of nanoparticles [8]. This is why colloidal gold nanoparticles with different size represent different colors. Scattering cross section is defined as the ratio of the scattering power over incident wave intensity [9]:

$$\sigma_{scat} = \frac{P_{scat}}{I_{source}} \quad [m^2] \tag{2.21}$$

Absorption cross section is the ratio of the absorbed power over incident wave intensity:

$$\sigma_{abs} = \frac{P_{abs}}{I_{source}} \quad [m^2] \tag{2.22}$$

The summation of absorption and scattering is called extinction:

$$\sigma_{extinction} = \sigma_{absorption} + \sigma_{scattering} \tag{2.23}$$

For sphere with the size a, scattering and absorption cross section is [3]:

$$\sigma_{sca} = \frac{k^4}{6\pi} |\alpha|^2 = \frac{8\pi}{3} k^4 a^6 |\frac{\varepsilon - \varepsilon_m}{\varepsilon + 2\varepsilon_m}|^2 \quad [m^2] \tag{2.24}$$

$$\sigma_{abs} = k \,\mathrm{Im}[\alpha] = 4\pi k a^3 \,\mathrm{Im}[\frac{\varepsilon - \varepsilon_m}{\varepsilon + 2\varepsilon_m}] \quad [m^2] \tag{2.25}$$

The above formula shows that scattering and absorption are related to the sixth and third power of spheres radius respectively. This means that with further decrease of nano particle size (r <50nm for gold or silver), absorption is going to be dominant factor over scattering [2].

Resonance frequency of a single nanoparticle is highly dependent to the nanoparticle's shape, dimensions, metal type and surrounding medium permittivity. By changing any of these items a shift in the resonance frequency would occur. For instance, increasing the amount of refractive index around the nanoparticles results in a red shift (shift towards bigger wavelengths) in the resonance frequency. This is actually the reason that there is interest in using plasmonic nanoparticles in biomedical field in detection of biomolecules, since each molecule represents a different refractive index. Increasing the amount of

electric field makes these nanoparticles more sensitive to the changes in the refractive indices which leads to a bigger shift in the resonance peak.

The challenge is to find a proper nanoparticle shape and structure that causes the highest amount of electric field created in its vicinity and increase. Many different figures such as sphere, disc, cube, pyramid, rod and star have been studied and fabricated to measure the peak resonance and also the amount of shift after exposure to biomolecules[10]. For example, spherical nanoparticles show a shift of 60nms per refractive index unit(RIU) whether this number for nanorods is around 250nm per RIU [10].

# Chapter 3: Plasmonic Sensors in the Literature

This chapter provides with the previous studies of researchers on the field of nano plasmonic and possible ways to enhance the sensitivity of these sensors.

## 3.1 Plasmonic in Sensing

The sensitivity of a plasmonic sensor is defined as

$$S = \frac{d\lambda_p}{dn} \tag{3.1}$$

in which $\lambda_p$ is the peak resonance wavelength and n is the refractive index of the surrounding medium [4]. Although increasing the length of the nanoparticle would increase its sensitivity, it will also make a wider linewidth that is the measured width at the half of the peak value[11]. For instance, nanorods have a smaller linewidth in comparison to nanospheres [12]. In order to include the effect of linewidth in the measurements, another expression with the name of figure of merit (FOM) is introduced [13]:

$$FOM = \frac{S}{\Gamma} \tag{3.2}$$

S is the sensitivity of the sensor.

$\Gamma$ is defined as the linewidth.

For comparison, nanoprisms show a typical figure of merit of 3 while for silver nanocubes this number is 5 [13].

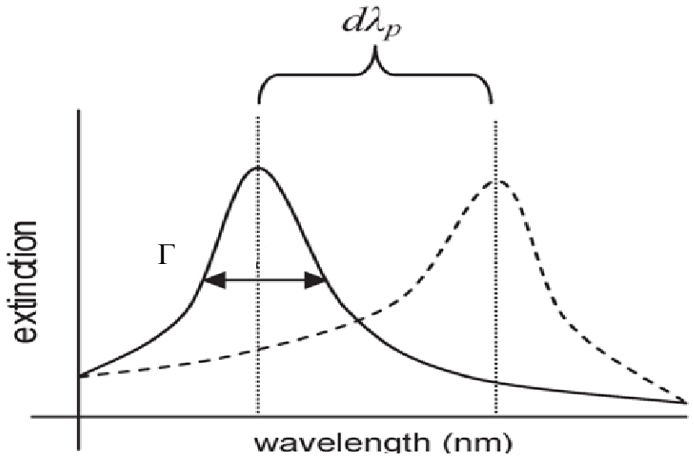


**Figure 3.1 Definition of linewidth( Γ ) and shift in the peak resonance[4]**

Experiments show that if nanoparticles are put close together with a small gap in between them, this would lead to a magnified electric field.

Van Duyne group used nanotriangles placed in a circular formation using nanosphere lithography (NSL). In this method in the first step, polymer nanosphere are placed tangentially together on a substrate. Then, a sheet of silver with the thickness of 50 nanometers is deposited on the structure. Finally, the polymer nanospheres are removed from the structure. This way, the filled triangular gaps among spheres with silver remain on the substrate[14], [15].

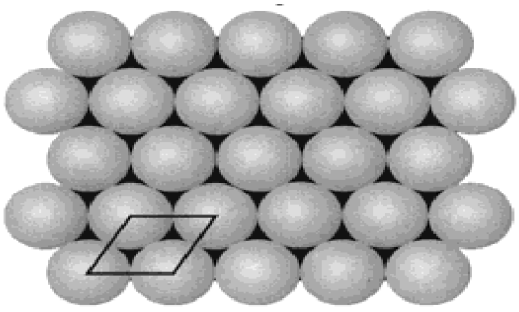

**Figure 3.2 Nanospherical polymers before metal deposition[14]**

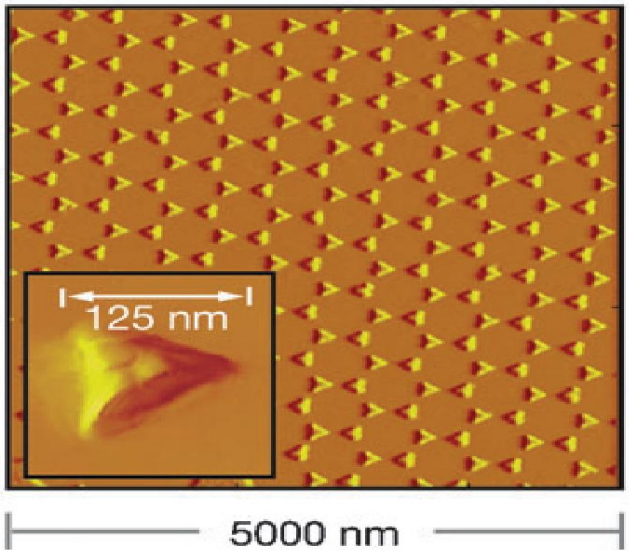


**Figure 3.3 Silver nanotriangles with the circular structure[5]**

Being inexpensive is one of the advantages this technique. In addition, this structure has a higher sensitivity than nanospheres[5],[1]. However, the created shapes are not exact triangles with the sharp edges and the produced extinction graph shows a wide linewidth in the resonance peak. Moreover, dimensions and the distance among the nanoparticles are approximate. Therefore, make it difficult to study the effect of size and distance on the resonance wavelength [5],[15]. The discussed structure was used to see the resonance peak of nitrogen, acetone, methylenechloride, cyclohexane, and pyridine.

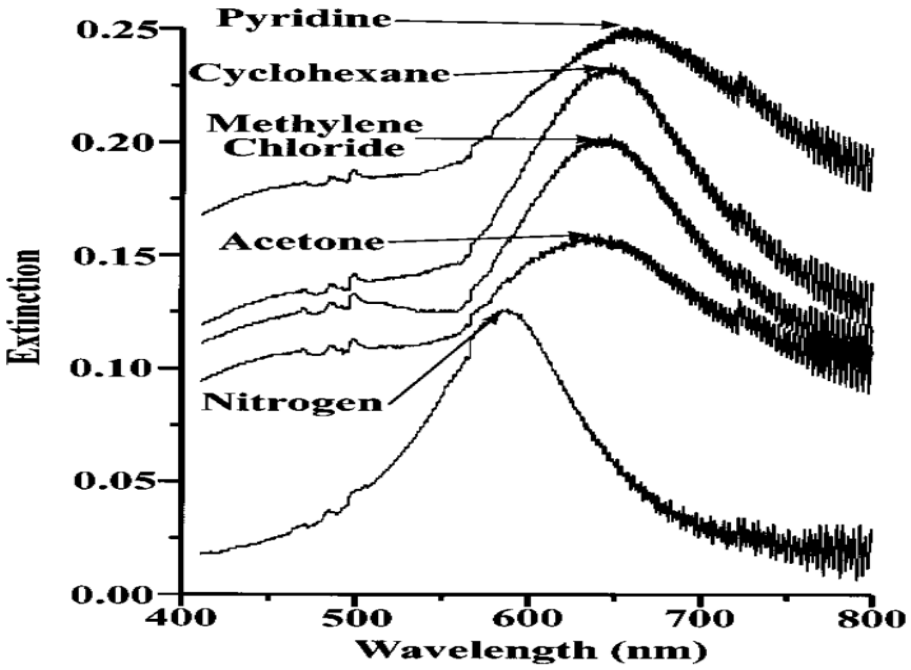


**Figure 3.4 Red shift in the resonance peak for chemicals with different refractive index [14].**

Due to high amount of electric field nanocubes and nanobars are also getting popular in recent research. In order to further increase the amount of nanoparticles colloidal structures are also proposed in which nanoparticle are floated inside a liquid. The advantage of colloidal nanoparticles is that it has a cheap and less complex fabrication process. However, because of random positioning of nanoparticles it is hard to study their characteristic and measure their sensitivity with precision [8]. One of the approaches that has gain attention is using of two nanorods placed with a small gap of a few nanometers. This structure because of its good ability to enhance absorption and scattering in the resonance frequency is called nanoantenna [2].

## 3.2 Enhancing The Resonance Shift

The relation between the shift in resonance peak and the difference in refractive index is described as [5],[1]:

$$\Delta\lambda \approx m(n_{adsorbate} - n_{medium})(1 - e^{\frac{-2d}{l_d}}) \tag{3.3}$$

m: Bulk refractive-index sensitivity [nm/RIU]

$n_{adsorbate}$ : Refractive index of the adsorbed chemicals. [RIU]

$n_{medium}$ : Refractive index of the medium. [RIU]

d: thickness of the adsorbate layer. [nm]

$l_d$ : decay length of the EM wave. [nm]

The formula shows that items such as $\Delta n$ and d can be optimized by changing the thickness of the adsorbate layer or simply increasing the difference in the refractive indices. However, the only factors that are directly related to the nanoparticle characteristics are m and ld. So by enhancing the EM wave, increasing extinction peak and decreasing the spectral linewidth it is possible to increase the sensitivity. For instance, increasing the nanoparticle size leads to an increase in “m” and “ld”. Also as mentioned earlier creating a small gap between nanoparticles creates a hot spot for the electric field.

## 3.3 Molecular Tuning

Research shows that increasing the size and mass of molecules lead to a bigger amount of shift in the resonance frequency[16]. In addition, if the chromophore of the molecule (chromophore is the part of a molecule responsible for its color) overlaps with the peak absorbance wavelength of the nanoparticle, there is higher spectral shift [1],[8]. Furthermore, Haes and Van Duyne, showed that when the thickness of the adsorbate layer reaches to 20 nm the detection sensitivity would decrease [15],[16].

One of the methods that is used for increasing the sensitivity of nanoparticles is by use of graphene. Coating of nanoparticles with graphene leads to a charge transfer between the nanoparticle and contributes to creation of a stronger electric field around the nanoparticle. This method has another advantage as well. Silver nanoparticles create a higher resonance peak than any other metal since their dielectric function has a large negative real and a smaller imaginary parts, but they are prone to oxidation which would reduce their sensitivity and therefore they are not as suitable as gold[17]. However, Choi et al mentions that coated silver with graphene is less subjected to oxidation [18].

## 3.4 Surface Enhanced Raman Scattering

Raman Scattering is a phenomenon discovered by C.V Raman who was awarded in 1930 with a Nobel Prize in physics. In his discovery, he realized that when light pass through a transparent substance a fraction of scattered light has been shifted in frequency in comparison to the incident light that is due to a difference in vibrational energy levels of the experimented molecules [19].

Each material has its specific Raman spectrum which is like a chemical fingerprint. The outcome of this method is used to identify molecules. However, one disadvantage of the Raman spectroscopy is the weak Raman emission which makes it hard to detect.

An alternate method to increase Raman scattering is called Surface Enhanced Raman Scattering(SERS). In this procedure, experimented molecules are placed in the proximity of metallic nanoparticles[20]. The plasmonic resonance of the nanoparticles that leads to a highly localized electric field, helps to enhance the Raman scattering by a factor of $10^6$ for concentrated amount of molecules [21]. Researchers are trying to push the SERS detection limit to a single molecule [22]. Nie and Emory used the SERS experiment for a single molecule of rhodamine 6G (a fluorescent dye) and reach to the enhancement factor of $10^{15}$ [21].

Application of SERS for real-time glucose measurement has also been studied [23],[24]. One of the challenges for LSPR sensing is that some molecules such as glucose show lower adsorption to the surface of nanoparticles. In addition, it is important to be able to isolate the target molecule from other substances in a solution. Coating the nanoparticles with chemical sensitive to the target molecules helps overcome this issue. This way, not only we can increase the adsorption, but also we can prevent binding of unwanted substances to the nanoparticle surface[1].

# Chapter 4: Simulation and Results

In this chapter we are going to use FDTD to simulate different nanoparticles structures and find the most suitable one with the highest sensitivity.

## 4.1 Simulation

In the previous chapter it was shown that by deploying Mie equation for metallic nanoparticles with spherical shapes the resonance frequency and the electric field could be driven. However, except for spheres and elliptical shapes, there is no comprehensive way to analyze other geometrical shapes. In addition, performing pure experimentation for measuring the results in the lab is costly and takes a lot of time as well. A better approach is by use of a Finite Difference Time Domain (FDTD) software, in which Maxwell equations are numerically solved in each region of the simulation. Therefore, Lumerical (FDTD) that is a pioneer software in the field of optics is employed to help us determine the plasmonic frequency for nanoparticles and be able to optimize our design.

Before going into the detail of the simulated nanoparticle structures, a brief explanation of the different elements of the software and their function is presented.

1. Source: we can choose different types of light source for our simulation such as Gaussian beam, Dipole beam and plain wave. Here a special type of plain wave, Total Field Scatter Field (TFSF), suitable for plasmonic simulation is chosen.
2. Cross section Monitor: This monitor measures the rate of absorbed or scatter power by the nanoparticle. By putting two Cross Section Monitors, one within the nanoparticle and the light source and the other outside the light source, total and scattering cross sections at each frequency is calculated.

3. Field Monitor: This monitor shows the localized electromagnetic field surrounding the nanoparticle as a function of wavelength or frequency.
4. Mesh Override Region: Mesh Override Region is a very important feature of the software in which by creating smaller regions for solving Maxwell equations, it generates a more precise result for the resonance frequency. A 2 nm meshing precision is chosen for the simulations.
5. FDTD: Shows the overall surrounding simulation region. Anything outside this region won't affect the simulation.

After simulation, by programming the script editor, a graph of the light extinction (extinction= scattered filed +total field) and its sensitivity to the shape and size of the nanoparticles could be demonstrated.

As we mentioned earlier the desired metal used to create plasmons is gold; because it's resonant peak lies in the visible spectrum of light and it is resistant to rust or chemical reactions while getting exposed to the fluids. In addition, it shows the highest extinction peak after silver among metals.

The purpose of this chapter is to simulate some of the famous nanoparticle shapes to see which structure creates higher electric field and therefore is more sensitive. Also we want to know the optimized dimensions of the nanoparticle.

## 4.2 Nanotriangle array

One of the proposed nanoparticles structures that is experimented by Van Duyne's group is made of silver nanotriangles with the width of 100 nm and the thickness of 50 nm [15],[14].The sharp edges of triangles are placed close together. It is worth mentioning that

the size and placing of these triangular nanoparticles in the fabrication is approximate. Figure3.1 shows the same simulation interface with the average spacing of 50 nm among the gold nanotriangles.

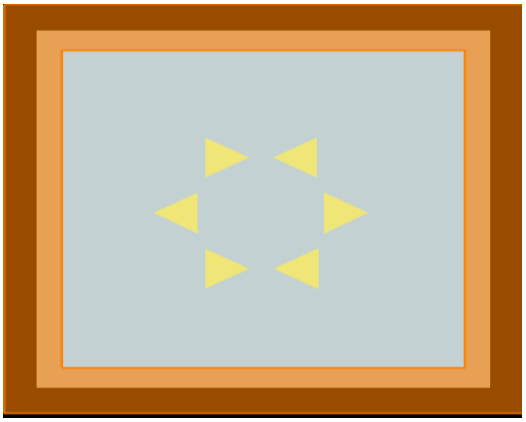

**Figure 4.1 Simulation interface for gold nanotriangles using FDTD**

The resonance frequency happens at $\lambda$ = 656 nm, that is at the red spectrum of the visible light. This structure creates a good amount of electric field in comparison to a single nanoparticle, but it also has a wide linewidth in the resonance frequency.

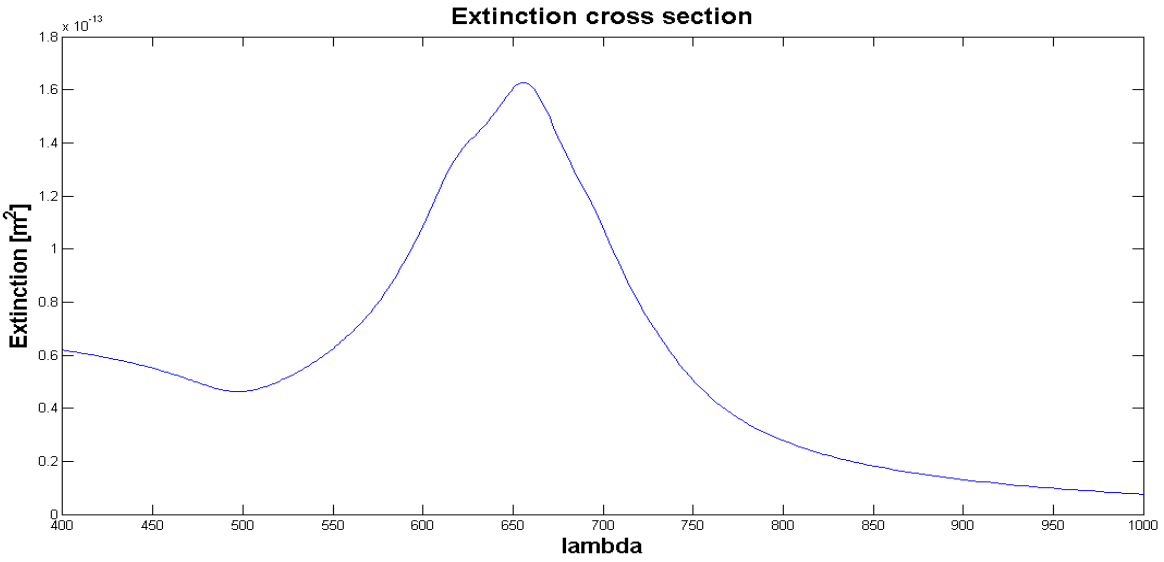


**Figure 4.2 Extinction cross section.** $\lambda_p = 657$ **nm**

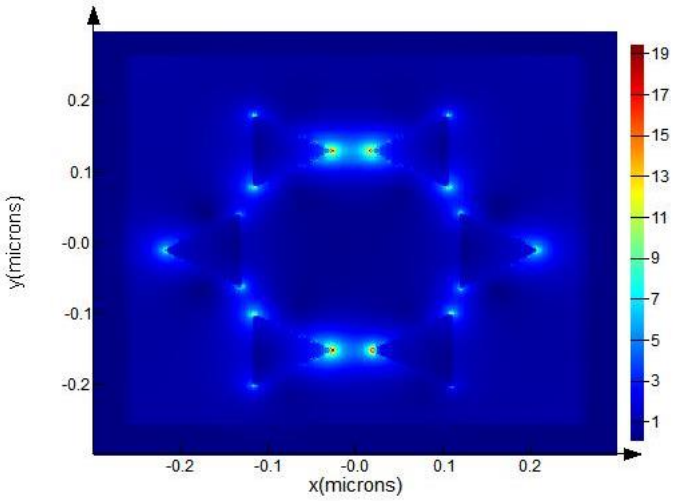


**Figure 4.3 Electric filed enhancement at the resonance frequency**

We can see the highest amount of electric field is at the sharp edges of this structure with the value of approximately 19 times of the electric field of the incident light.

Extinction cross section shows the effective area of the electromagnetic field when interacting with nanoparticles. Higher number for extinction makes detection easier.

Another expression that helps understand extinction better is called efficiency factor (Q).

Q is defined as the ratio of EM cross-section to the physical cross section of the particle[2].

$$Q_{ext} = \frac{\sigma_{ext}}{area} \tag{4.1}$$

For example, Q=5 reveals that the created field around the nanopariticle is 5 times bigger than its physical cross section. It is also known as Mie efficiency.

## 4.3 Nanoantenna

Another structure that has gained popularity is nanoantenna. Nanoantennas are made of two nano bars which are placed close together[2]. Research shows that having two

nanoparticles could create a higher electric field in comparison to a single nanoparticle[25]. This is a good out come because it would also increase the sensitivity of the sensor. Here, the simulation with a sweep of distance between two nanoparticles is shown. The two nanobars are symmetrical each with a width of 50 nm, thickness of 30 nm and length of 100 nm. The distance between the two nano bars is swept from 50 nm down to zero nm with a 12.5 nm steps. We can see that by decreasing the distance we have a red shift in the resonance frequency and a growth in the electric field is observable.

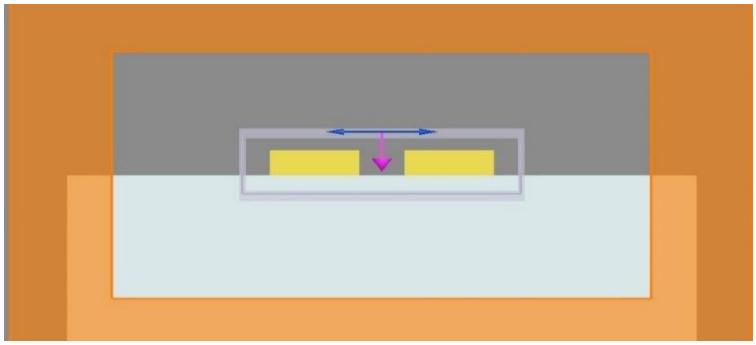

**Figure 4.4 Simulation of nanoantenna. Incident light is polarized at the x direction**

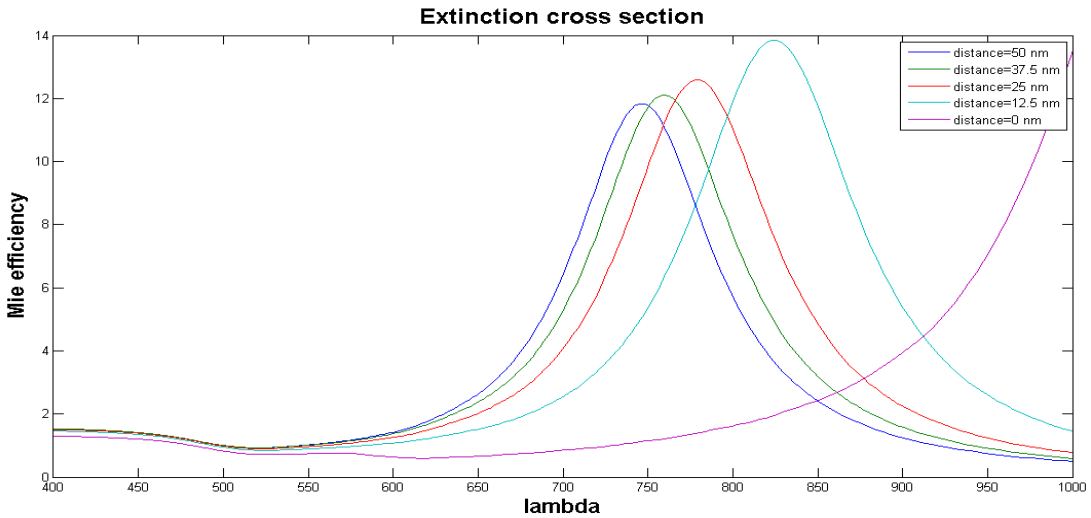


**Figure 4.5 Nanoantenna distance sweep. Reducing the distance in nanoantenna leads to red shift in peak resonance**

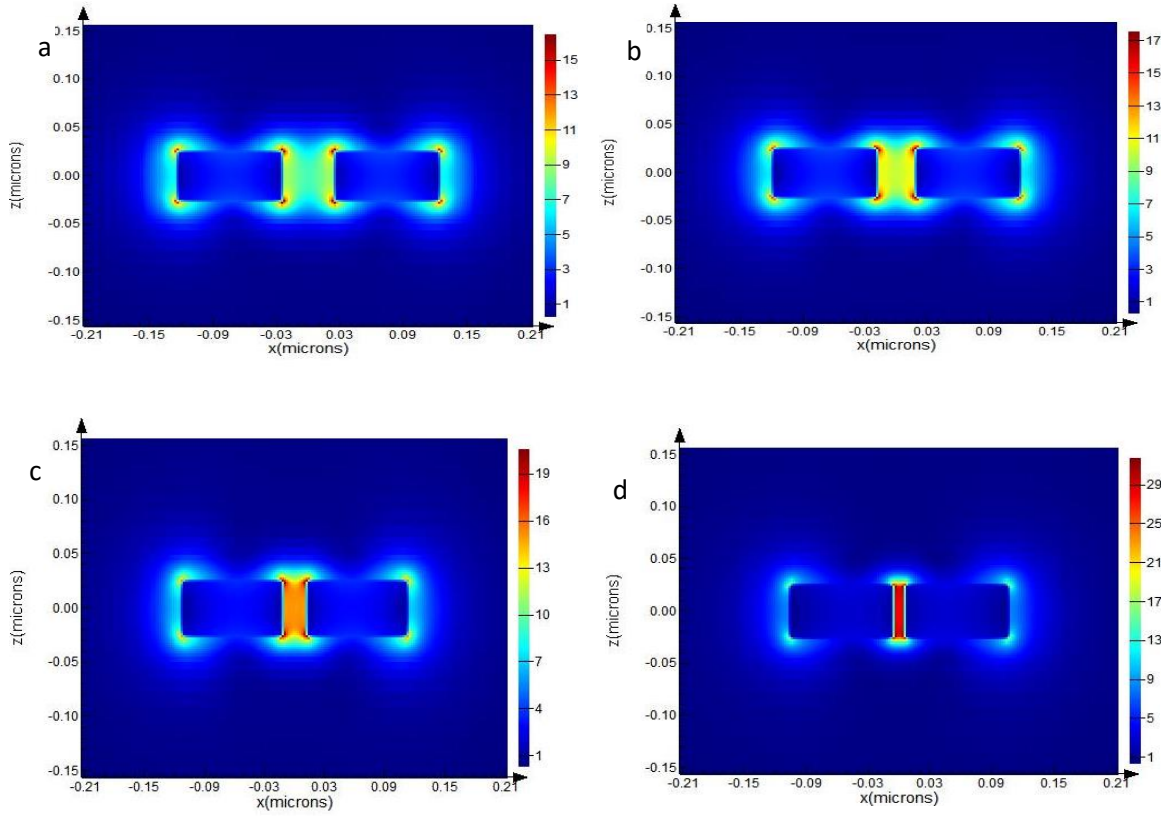


**Figure 4.6 Impact of distance on the electric field coupling**

Figure 3.6 shows that decreasing the distance between nanoparticles results in an increase in the electric field coupling from 15 to 29 times of the incident wave.

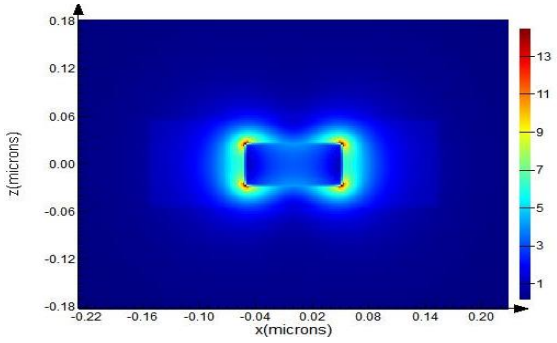


**Figure 4.7 Single nanobar field enhancement**

In the next experiment in order to see the effect of dimensions on the extinction, resonance frequency and the electromagnetic filed; distance between nanobars are kept constant to 50 nm and length, width and thickness of the nanoantennas where altered.

### 4.3.1 Sweeping Length

In this section, length of the nano bars were changed from 75 nm to 125 nm. Figure below shows that increasing the size of nanobars not only causes a redshift, but also contributes to the Mie efficiency. However, increasing the length has the drawback of increasing the linewidth at resonance frequency that makes it not suitable for sensing purposes.

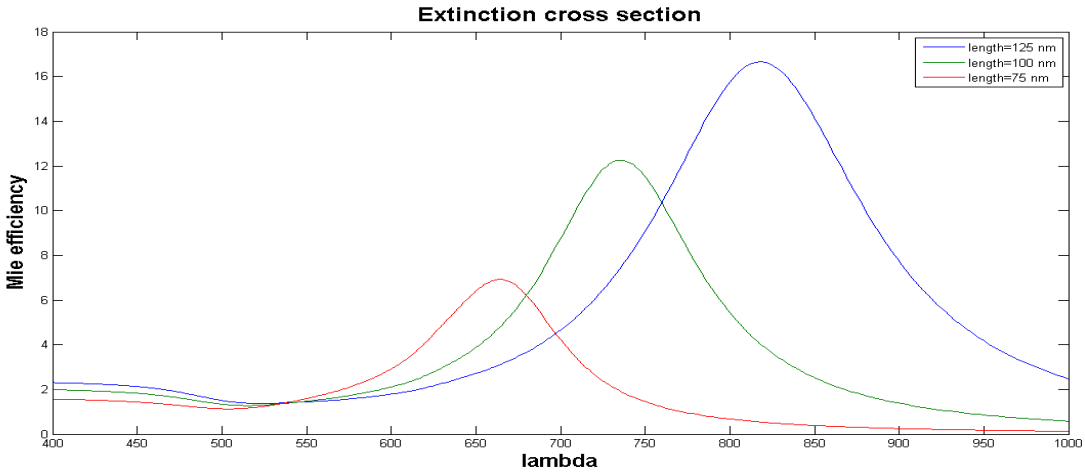


**Figure 4.8 Increasing the nanoantenna's length**

### 4.3.2 Sweeping Width

In this experiment width of the nanobars were increased from 30 nm to 50 nm. In contrast to the previous section, increasing width creates a blue shift in the resonance peak. But the efficiency approximately remains unchanged. In addition, the localized electric field is reduced from 17 to 13.

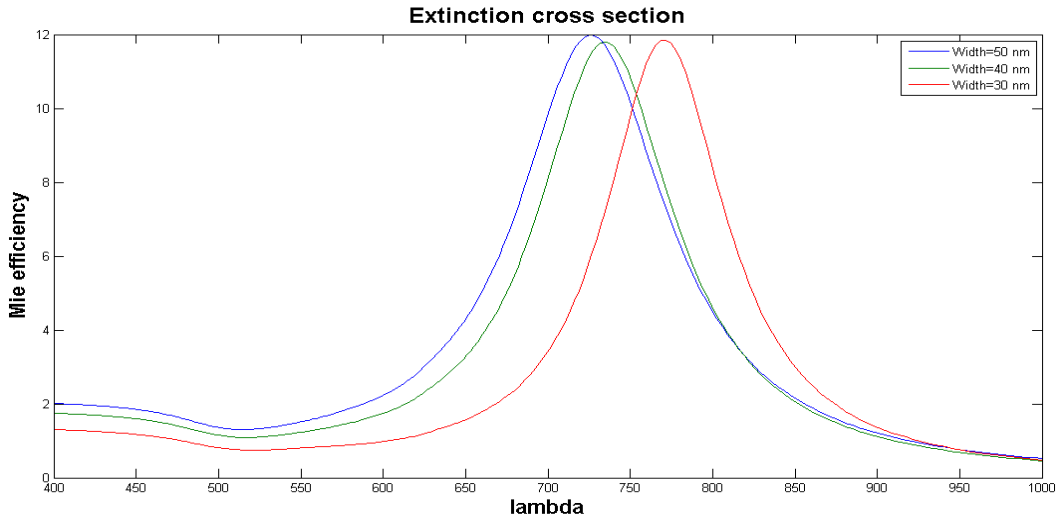


**Figure 4.9 Increasing the nanoantenna's width**

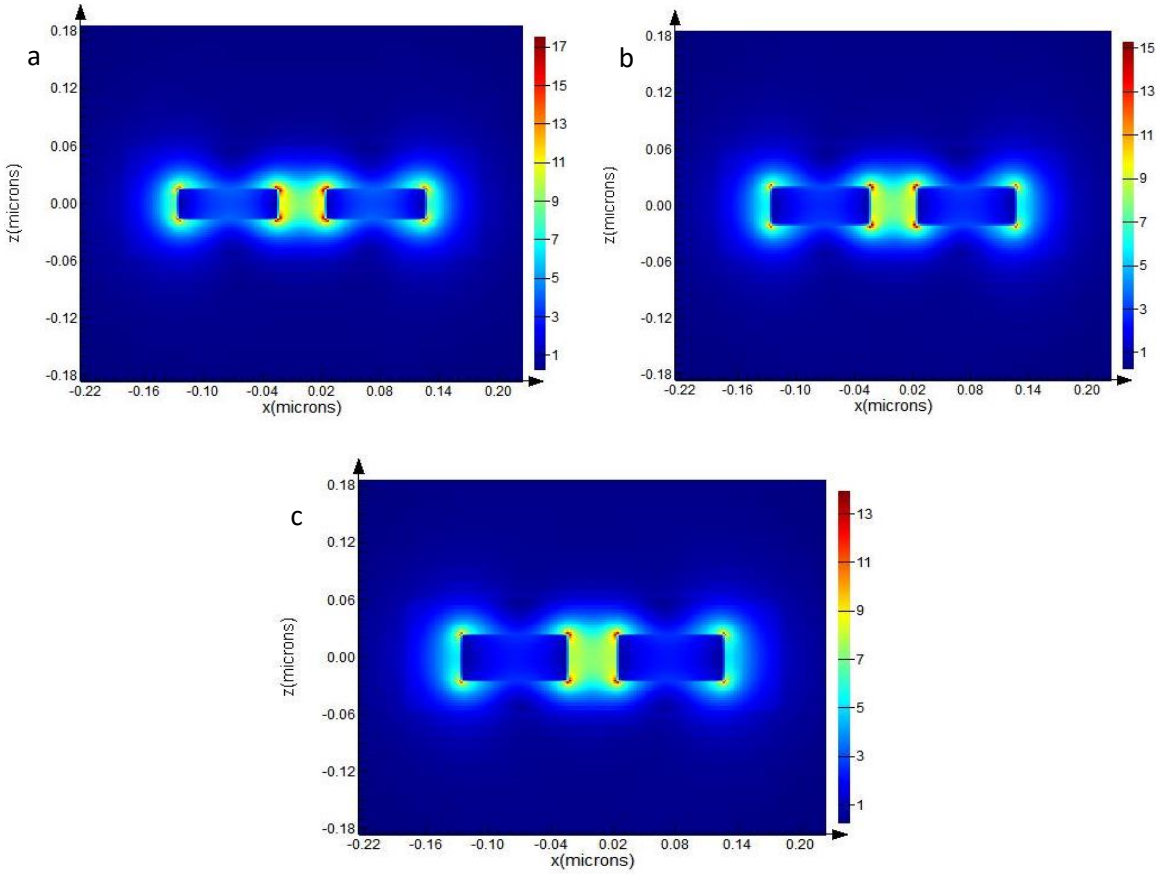


**Figure 4.10 Effect of width in the field enhancement. a) width=30nm b) width=40 nm c) width=50tnm**

### 4.3.3 Sweeping Thickness

Similar to the previous part changing the thickness from 20 nm to 40nm would again result in a blue shift in the resonance peak and causes a lower electric field. Results of figure 4.11 and 4.12 suggests to keep thickness as small as possible.

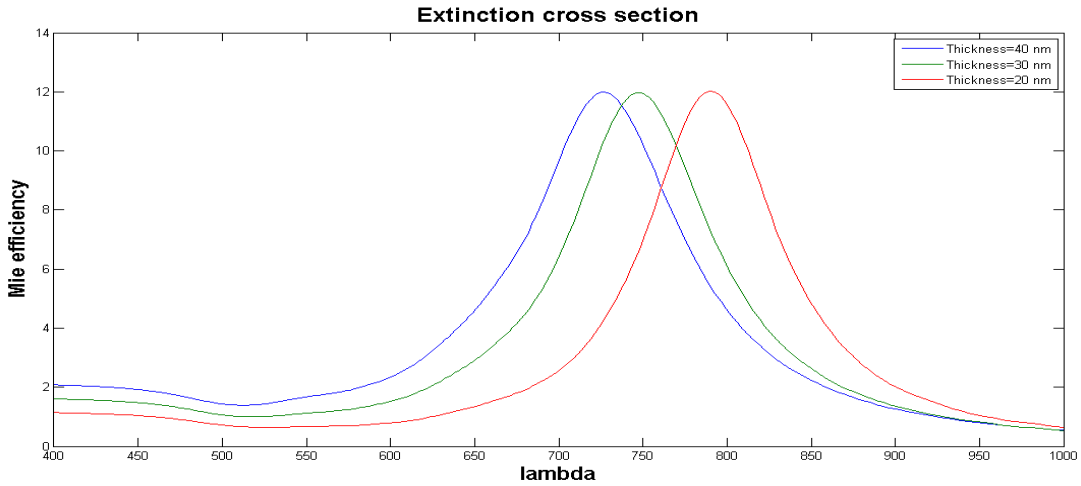


**Figure 4.11 Effect of thickness in the resonance peak**

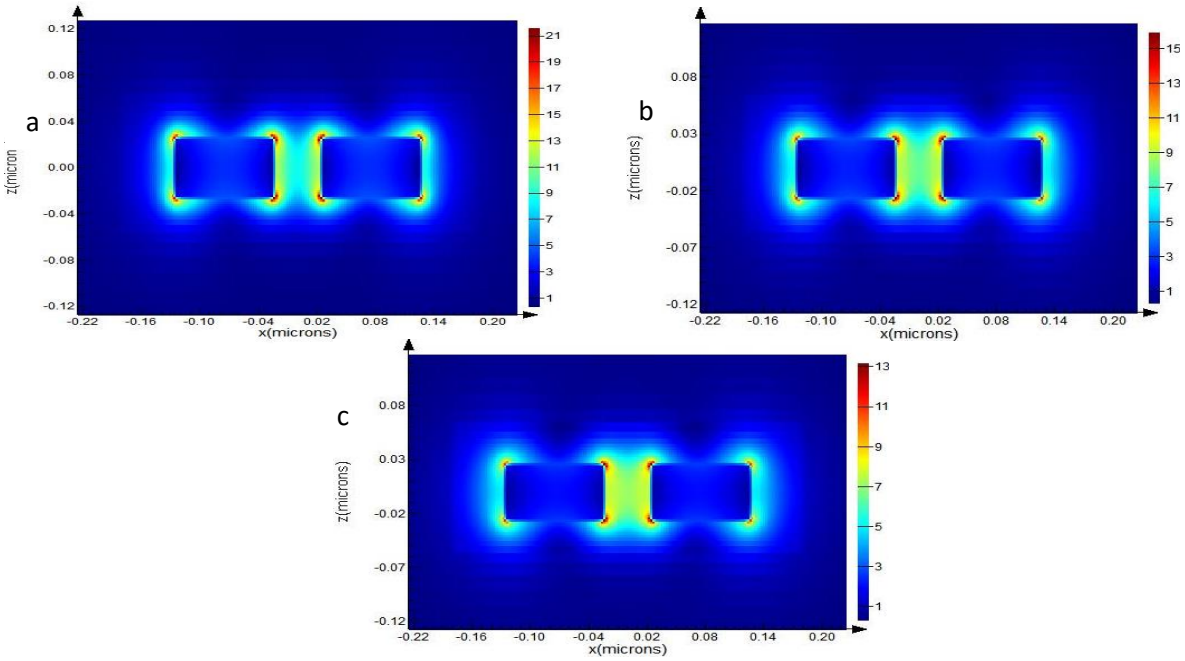


**Figure 4.12 Thickness effect in the electric field. Increasing the thickness, attenuates the electric field coupling. a) z=20 nm b) z=30 nm c) z=40 nm**

These experiments show that to reach the highest electric field it is better to reduce the thickness and width of the nanobars and instead increase the length to the point that the linewidth of peak resonance is acceptable.

As it is mentioned earlier extinction is the summation of scattering and absorption of light by nanoparticles. Experiment shows that regardless of the shape of a nanoparticle, decreasing its dimensions would also decrease the light scattering and at the same time increase the absorption[2],[1]. On the other hand, some spectroscopy devices such as dark field spectroscopy are used to measure light scattering and as a result it might not be possible to decrease the nanoparticle's dimensions and thus scattering behind their detection limit. Figure 4.13 shows the absorption and scattering cross section for the previous simulation. We can see that increasing the thickness of nanobars from 20 nm to 40 nm leads to a higher scattering but a lower absorption efficiency.

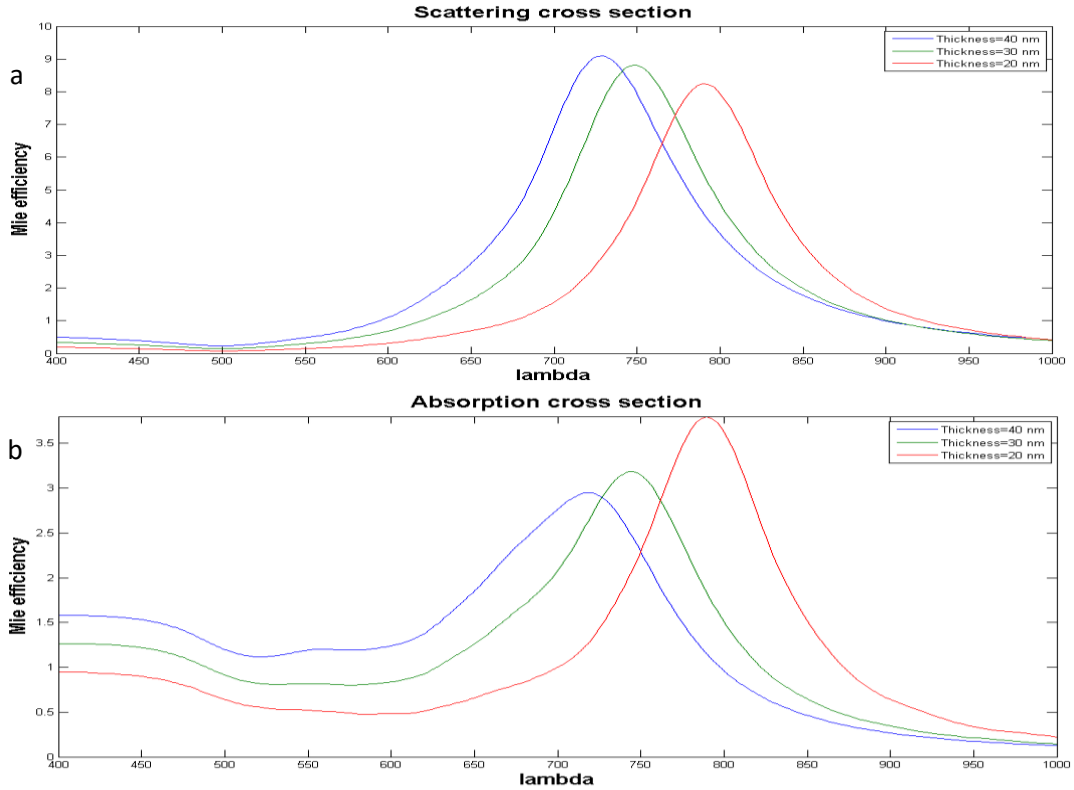


**Figure 4.13 relation between scattering and absorption cross section**

## 4.4 Bow tie

The other sturcture that is studied is bow tie. The pupose of this simulation is to see if having sharp edges is going to contribute to a more focused and enhanced electric field.

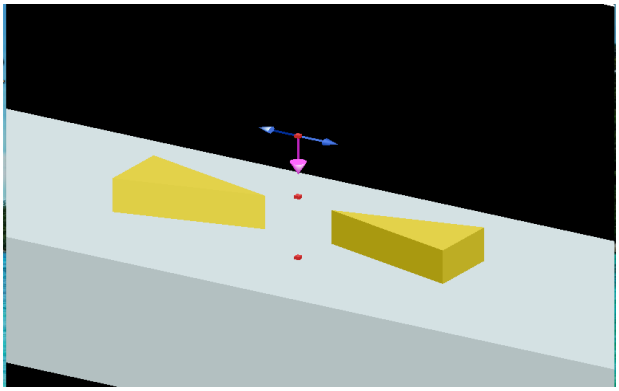

**Figure 4.14 Bow tie perspective view. Incident light is polarized in the x axis**

Similar to previous simulation of nanobars, enlarging the length of nanotriangles in the x-y plane causes a red shift with a wider linewidth and a higher electric field. Increasing the thickness of nanotriangles also shows a blue shift in peak resonance and also a reduction in the electric field. Changing the base of these nanotriangles would also change the sharpness of their tips. In this simulation, the base of nanotriangles are changed from 50 to 30 nm.

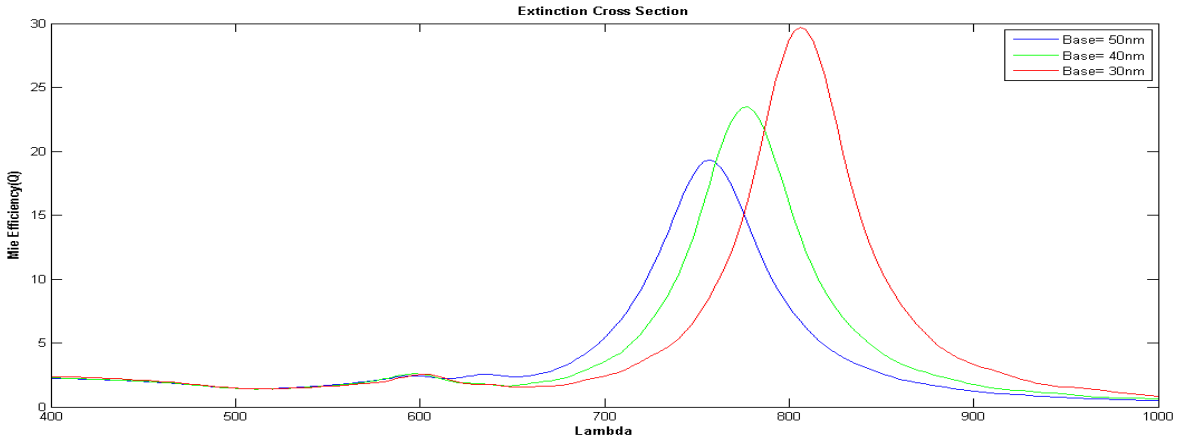


**Figure 4.15 Relation between base and the resonance peak. Smaller base creates smaller angle inside the bow tie and a sharper edge on the outside.**

Figure above shows that by having a sharper tip at base size of 30 nm there is a red shift in the resonance peak and an intensified electric field between the two nanotriangles. It is notable that not only a bowtie structure shows a more enhanced field in comparison to nanoantenna, but also they have a narrower linewidth in the peak resonance. The calculated linewidth for nanoantenna is approximately 110 nm whether this value for bow tie is 70nm.

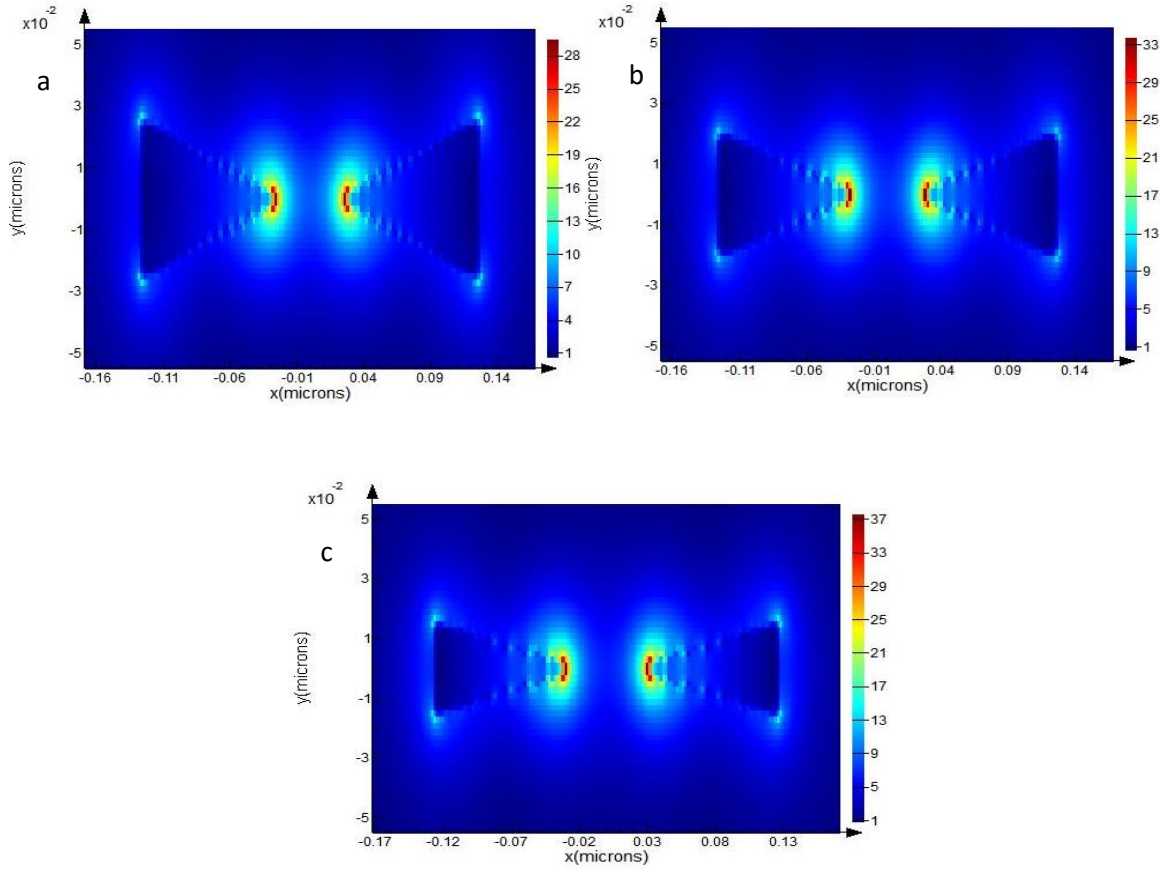


**Figure 4.16 Decreasing base size from 50 nm to 30 nm creates higher electric filed**

Finally, in this section a distance sweep between the two nanotriangles has been carried out. Both nanotriangles have the length of 100 nm, base of 50 nm and thickness of 30 nm.

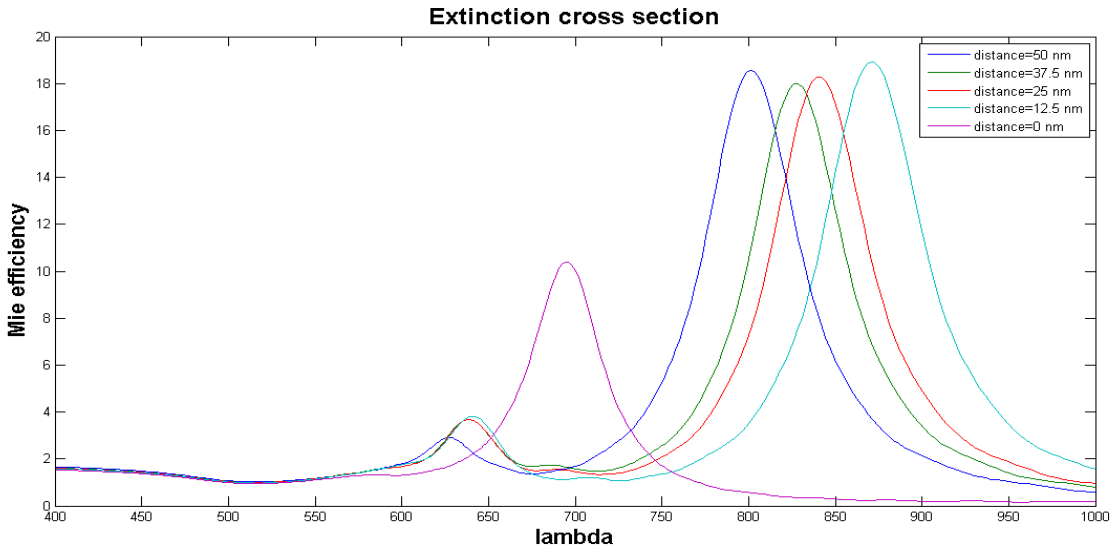


**Figure 4.17 Bow tie distance sweep**

Decreasing distance creates a red shift (higher electric field). However, at distance zero there is no coupling between nanoparticles and there is a blue shift. One of the interesting results of narrowing the gap in the bow tie structure is that the field enhancement is more sensitive to the smaller than 25nm gap variations than in the nanoantenna. For instance, in figure 4.6 (c) and (d), closing the gap from 25 nm to 12.5 nm in nanoantenna results in a difference of 10 times in filed improvement whether for bow tie in the figure 4.18(c) and (d) with the exact distance variation this number is approximately 25 times of enhancement.

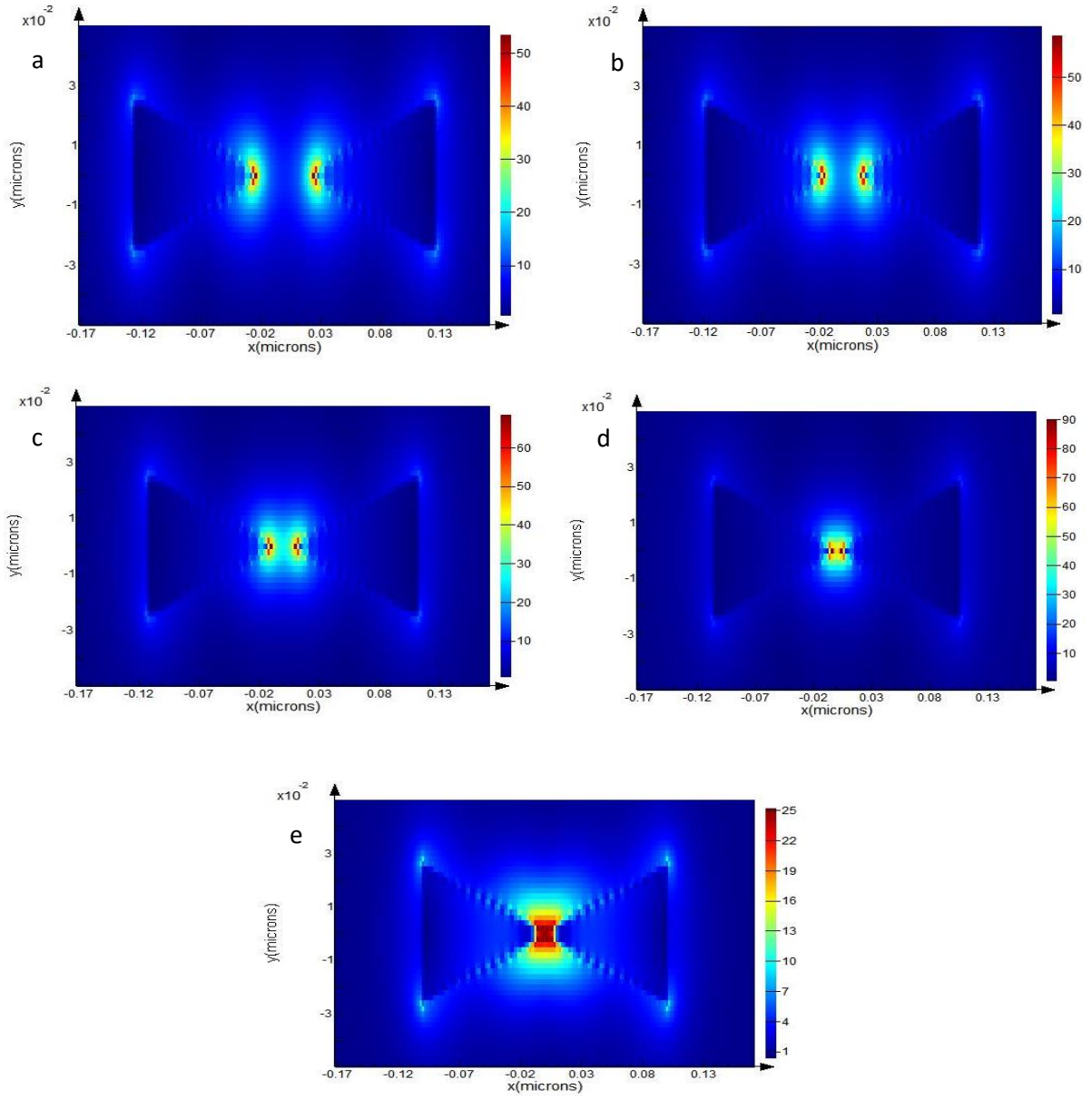


**Figure 4.18 Effect of distance on enhancing electric field in the bow tie structure**

Figure 4.18 illustrates that it is possible to reach an electric field magnitude of 90 times of the incident light at the distance of 12.5 nm. Although nanotriangles create a more intensified electric field than nanobars, however, this field decays faster than nanobars and is not suitable for our biomolecule detecting purpose. To solve this issue, it is better to put nanotirangles in distances smaller than 25 nm.

## 4.5 Dielectric

After performing the simulation for two different structures and doing the dimension sweep to see the optimum size for both bow tie and nanobars, in this part a dielectric is placed in the gap between the nanoparticles to see its effect on the resonance peak. A sphere shaped water with a radius of 10 nm is used as a dielectric. Therefore, volume of the water is approximately $4.19\times10^{-12}$ nanoliter that is equal to two and a half million water molecules. The suggested bow tie has a length, base and thickness 100 nm, 50 nm and 30 nm respectively. Moreover, the gap in the bowtie structure is 20 nm. (viruses have a diameter of 20 to 300 nm.)

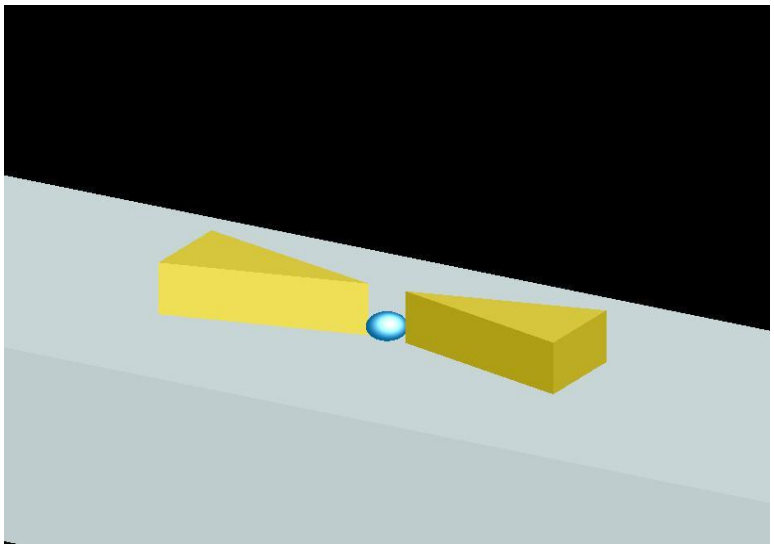

**Figure 4.19 Water nanosphere in the middle of bow tie structure**

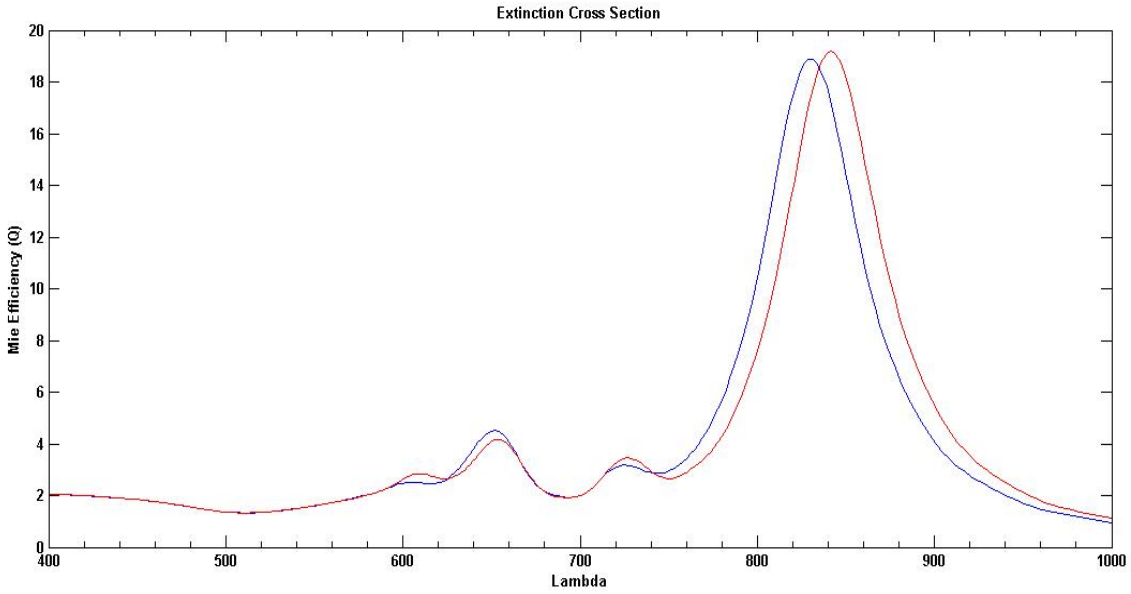


**Figure 4.20 Red shift after placing water**

The extinction cross section graph shows that there is a red shift in frequency from 831.3 nm to 841.8 nm ( $\Delta\lambda = 10.5$ nm).

The same simulation was implemented for the nanoantenna structure with the dimension of length:100nm, width: 50nm, thickness:30 nm and gap size of 20 nm.

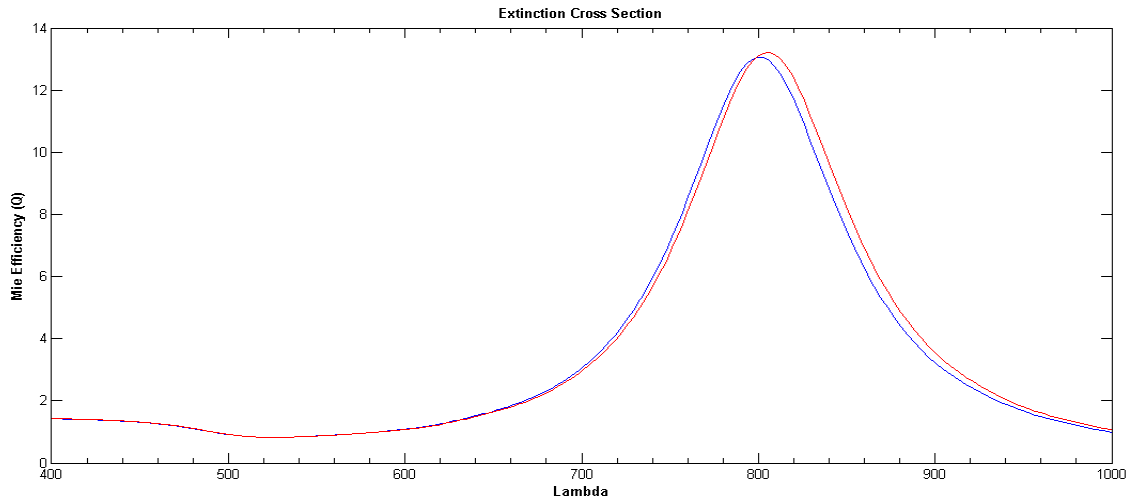


**Figure 4.21 Water nanosphere in the middle of nanoantenna**

After exposing to a sphere made of water, the nanoantenna structure shows a red shift in the resonance peak from 799.5 to 805.29 nm ( $\Delta\lambda = 5.79$ nm).

# Chapter 5: Application

In this chapter several applications of the nano plasmonic sensors and their advantages in other fields has been described.

## 5.1 Gas sensor

Cheng et al. used silver nanoparticles and gold nanoshells for detection of chemical vapors such as toluene (a derivative of Benzene) with the detection limit of 5ppm. [26] Their gold nanoshells showed a red shift of 250 (nm/RIU) when placed close to organic vapors.

In another study, Liu et al. have created a structure made of a gold nanotriangle in the neighborhood of a palladium nanodisc for indirect hydrogen detection[27]. In this structure palladium acts as a catalyst and make a reaction with hydrogen that leads to palladium hydride. This changes the refractive index of the palladium. The structure was made of two gas channels of nitrogen and hydrogen. In the experiment the sensor was able to make a 5 nm resonance red shift at 1% concentration of hydrogen in the gas flow controller.

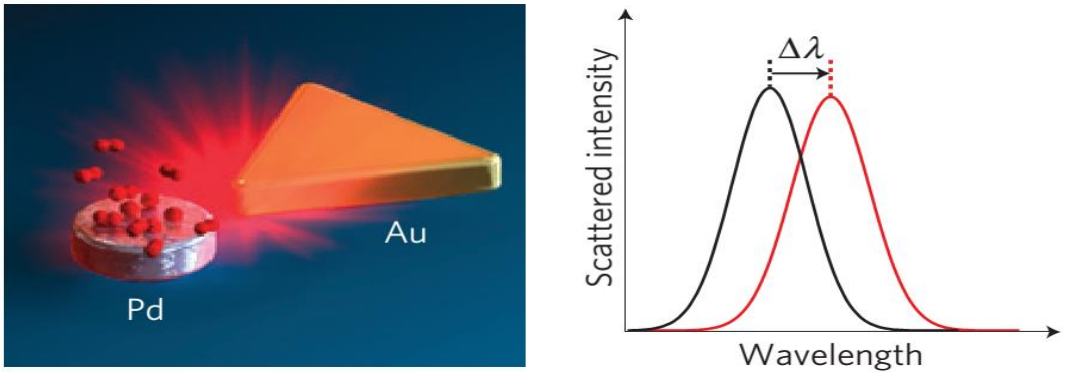


**Figure 5.1 Hydrogen gas detection[27]**

## 5.2 PH sensor

Mack et al. created a plasmonic PH sensor in which nano particles were coated with a hydrogel sensitive to PH [28]. An increase to the PH of the medium would expand the volume of the hydrogel. This results in lowering the refractive index and a blue shift in the extinction. A precision of 0.1 PH within the range of 1.44 up to 7.86 has been achieved for this method.

## 5.3 Multiplexing

The other advantage of LSPR sensors is multiplexing. By this mean several types of chemicals can be detected concurrently[4]. In this technique nanoparticles with different sizes are used so that each one would have a resonance peak at diverse frequencies in order not to interfere. This way it is possible to detect several targets in one solution [29].

Yu and Irudayaraj, created a plasmonic biosensor using nanorods with different dimensions to simultaneously measure three different antibodies [29].

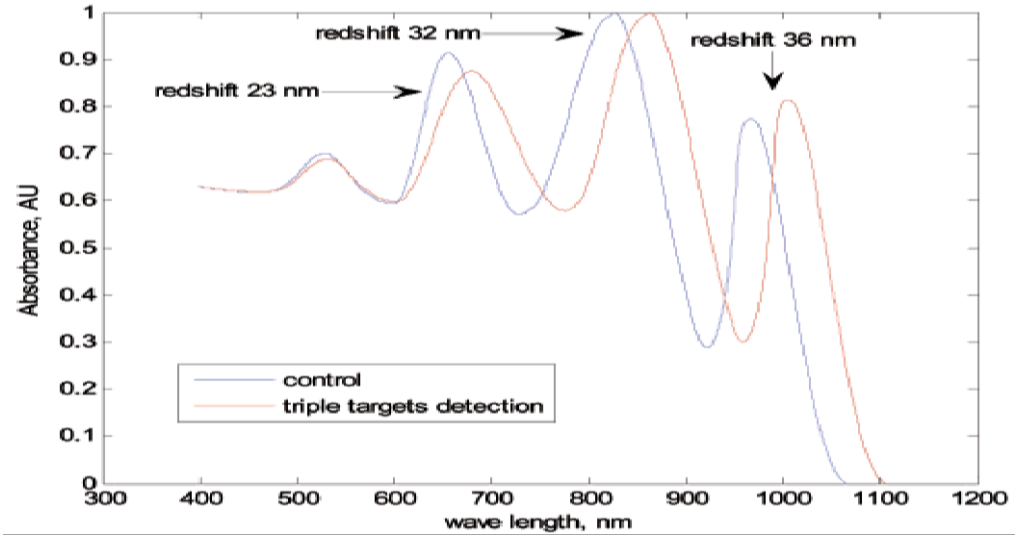


**Figure 5.2 Multiplexing in detection[29]**

## 5.4 Microfluidic Chip

In recent studies there have been some approaches to produce a low cost chip with a good amount of precision in order to make integrated lab on chip possible.

In this regard, Hiep et al. have presented a low cost microfluidic chip based on LSPR sensors[30]. The nanoparticles in the chip were made of spherical glass nanoparticle coated with gold layers. The chip was able to measure variations in the refractive index of glucose. In addition, the chip was used to calculate the antigen-antibody interaction time with the precision of 100ng/ml.

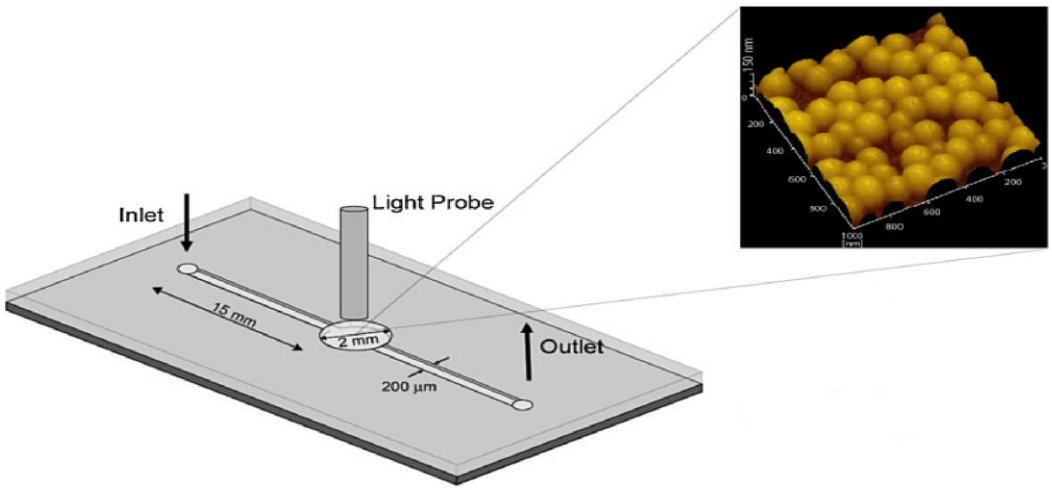


**Figure 5.3 Microfluidic chip**

In another study, Acimovic et al. introduced a chip made of nanorod with 8 independent channels for fast detection of cancer cells by measuring biomarkers of prostate cancer and was able to reach the detection limit of 500ng/ml [31].

## 5.5 Imaging and Treatment

In order to detect diseases like cancer, biomarkers (measurable indicator of a biological condition) and contrast agents are used. Fulfilling this method requires fluorescent dyes.

The flaw of this method is the photobleaching of these dyes in which they become unable to fluoresce. In contrast, nanoparticles do not photobleach [32].

In addition, nanoparticles can be used for photothermal imaging. Nanoparticles smaller than 20 nm have higher absorption than scattering[2]. This results in an increase in the temperature of the NP and the surrounding tissue as well [33].

NPs have also been deployed in medical treatment. Resonance frequency of NPs can be tuned into certain frequency in which light can easily penetrated to the body and get absorbed by NPs and increasing the temperature to the point that could destroy cancer tumors [34],[35].

## 5.6 Solar cells

In recent years, solar cells have gained popularity among renewable sources for producing electricity. They are pollution free and could be easily installed in houses as a complement source of energy. However, they have higher costs than fossil-fuels and have low efficiencies to convert sunlight to electricity[36]. Photovoltaic cells are mostly made of crystalline silicon which consists most of the production cost. One proposed way to reduce the cost is to reduce the thickness of the silicon wafers from100-300 micrometer, to a few micrometers. Although this would reduce the cost, but it would also reduce the efficiency of solar cells. In order to solve this issue, Wang et al. deployed plasmonic nanoparticles to enhance the light absorption and were able to reach 30% improvement in the broad band absorption [37].

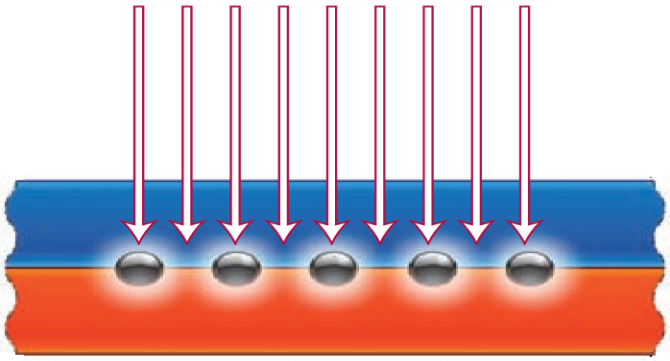

**Figure 5.4 Metallic nanoparticles in solar cells. Localized electric field around nanoparticles helps to produce electron-hole pairs[38].**

# Chapter 6: Conclusion

Because of the ability of metallic nanoparticles to absorb and scatter light coherently, they have been utilized in the other filed such as solar cells, for enhancing the efficiency of producing electricity; in thermal imaging for tracking the nanoparticles inside a living tissue or utilized in Surface Enhanced Raman Spectroscopy.

The scope of this thesis was about finding the appropriate structure and dimensions for nanoparticles that make them proper for bio-sensing.

Three different structure were examined. Nanoparticles with random spacing produce a good amount of electric field. However, they create wider linewidth in the resonance peak. Furthermore, since the nanoparticles arrangement is not exact in size and distance, the field is not equal through the whole structure. This property makes this configuration hard to study.

In the second approach, nanoantennas were simulated. It was shown that for a single nanobar, reducing the width and thickness while increasing the length leads to the highest amount of electric field. Moreover, making the gap smaller enhances the electric field as well.

In comparison to the nanoantenna, bow tie structure produces a higher amount of electric field that is because of the advantage of having sharp edges. Similar to nanoantenna, decreasing the thickness and the base of bowtie helps to have a higher electric filed. In addition, the resonance peak has a narrower linewidth that helps for an improved sensitivity. A phenomenon that is common in all experiments is that an increase in the electric field leads to a red shift in the peak resonance.

In the final experiment, a nanosphere with the radius of 10 nm and made of water was place in gap between the bowtie and nanoantenna to measure the amount of sensitivity. Simulation results showed that the bowtie structure made a 10.5 nm red shift in the resonance peak whether nanoantenna made a 5.8 nanometer shift. This proves that bow tie structure contributes to a higher amount of sensitivity and makes it a great candidate as a biosensor. Biosensing with LSPR sensors makes a label free, multiplexed and real time detection possible. In addition, the cheap fabrication price of these sensors demonstrates a promising future in the industry.

# References


[1] J. N. Anker, W. P. Hall, O. Lyandres, N. C. Shah, J. Zhao, and R. P. Van Duyne, "Biosensing with plasmonic nanosensors," *Nature materials,* vol. 7, pp. 442-453, 2008.

[2] V. Giannini, A. I. Fernández-Domínguez, S. C. Heck, and S. A. Maier, "Plasmonic nanoantennas: fundamentals and their use in controlling the radiative properties of nanoemitters," *Chemical reviews,* vol. 111, pp. 3888-3912, 2011.

[3] S. A. Maier, *Plasmonics: fundamentals and applications*: Springer Science & Business Media, 2007.

[4] K. M. Mayer and J. H. Hafner, "Localized surface plasmon resonance sensors," *Chemical reviews,* vol. 111, pp. 3828-3857, 2011.

[5] K. A. Willets and R. P. Van Duyne, "Localized surface plasmon resonance spectroscopy and sensing," *Annu. Rev. Phys. Chem.,* vol. 58, pp. 267-297, 2007.

[6] P. B. Johnson and R.-W. Christy, "Optical constants of the noble metals," *Physical review B,* vol. 6, p. 4370, 1972.

[7] G. Mie, "Beiträge zur Optik trüber Medien, speziell kolloidaler Metallösungen," *Annalen der physik,* vol. 330, pp. 377-445, 1908.

[8] E. Ringe, B. Sharma, A.-I. Henry, L. D. Marks, and R. P. Van Duyne, "Single nanoparticle plasmonics," *Physical Chemistry Chemical Physics,* vol. 15, pp. 4110-4129, 2013.

[9] C. F. Bohren and D. R. Huffman, *Absorption and scattering of light by small particles*: John Wiley & Sons, 2008.

[10] L. Guo, J. A. Jackman, H.-H. Yang, P. Chen, N.-J. Cho, and D.-H. Kim, "Strategies for enhancing the sensitivity of plasmonic nanosensors," *Nano Today,* vol. 10, pp. 213-239, 2015.

[11] J. Becker, A. Trügler, A. Jakab, U. Hohenester, and C. Sönnichsen, "The optimal aspect ratio of gold nanorods for plasmonic bio-sensing," *Plasmonics,* vol. 5, pp. 161-167, 2010.

[12] Y. Li, K. Zhao, H. Sobhani, K. Bao, and P. Nordlander, "Geometric dependence of the line width of localized surface plasmon resonances," *The journal of physical chemistry letters,* vol. 4, pp. 1352-1357, 2013.

[13] L. J. Sherry, S.-H. Chang, G. C. Schatz, R. P. Van Duyne, B. J. Wiley, and Y. Xia, "Localized surface plasmon resonance spectroscopy of single silver nanocubes," *Nano letters,* vol. 5, pp. 2034-2038, 2005.

[14] C. L. Haynes and R. P. Van Duyne, "Nanosphere lithography: a versatile nanofabrication tool for studies of size-dependent nanoparticle optics," *The Journal of Physical Chemistry B,* vol. 105, pp. 5599-5611, 2001.

[15] A. J. Haes and R. P. Van Duyne, "A unified view of propagating and localized surface plasmon resonance biosensors," *Analytical and bioanalytical chemistry,* vol. 379, pp. 920-930, 2004.

[16] A. J. Haes, S. Zou, G. C. Schatz, and R. P. Van Duyne, "Nanoscale optical biosensor: short range distance dependence of the localized surface plasmon resonance of noble metal nanoparticles," *The Journal of Physical Chemistry B,* vol. 108, pp. 6961-6968, 2004.

[17] G. J. Nusz, A. C. Curry, S. M. Marinakos, A. Wax, and A. Chilkoti, "Rational selection of gold nanorod geometry for label-free plasmonic biosensors," *Acs Nano*, vol. 3, pp. 795-806, 2009.

[18] S. H. Choi, Y. L. Kim, and K. M. Byun, "Graphene-on-silver substrates for sensitive surface plasmon resonance imaging biosensors," *Optics express*, vol. 19, pp. 458-466, 2011.

[19] C. V. Raman and K. S. Krishnan, "A new type of secondary radiation," *Nature*, vol. 121, pp. 501-502, 1928.

[20] A. R. Tao, S. Habas, and P. Yang, "Shape control of colloidal metal nanocrystals," *small*, vol. 4, pp. 310-325, 2008.

[21] S. Nie and S. R. Emory, "Probing single molecules and single nanoparticles by surface-enhanced Raman scattering," *science*, vol. 275, pp. 1102-1106, 1997.

[22] K. Kneipp, Y. Wang, H. Kneipp, L. T. Perelman, I. Itzkan, R. R. Dasari, *et al.*, "Single molecule detection using surface-enhanced Raman scattering (SERS)," *Physical review letters*, vol. 78, p. 1667, 1997.

[23] D. A. Stuart, J. M. Yuen, N. Shah, O. Lyandres, C. R. Yonzon, M. R. Glucksberg, *et al.*, "In vivo glucose measurement by surface-enhanced Raman spectroscopy," *Analytical chemistry*, vol. 78, pp. 7211-7215, 2006.

[24] O. Lyandres, N. C. Shah, C. R. Yonzon, J. T. Walsh, M. R. Glucksberg, and R. P. Van Duyne, "Real-time glucose sensing by surface-enhanced Raman spectroscopy in bovine plasma facilitated by a mixed decanethiol/mercaptohexanol partition layer," *Analytical chemistry*, vol. 77, pp. 6134-6139, 2005.

[25] P. Ghenuche, S. Cherukulappurath, T. H. Taminiau, N. F. van Hulst, and R. Quidant, "Spectroscopic mode mapping of resonant plasmon nanoantennas," *Physical review letters,* vol. 101, p. 116805, 2008.

[26] C.-S. Cheng, Y.-Q. Chen, and C.-J. Lu, "Organic vapour sensing using localized surface plasmon resonance spectrum of metallic nanoparticles self assemble monolayer," *Talanta,* vol. 73, pp. 358-365, 2007.

[27] N. Liu, M. L. Tang, M. Hentschel, H. Giessen, and A. P. Alivisatos, "Nanoantenna-enhanced gas sensing in a single tailored nanofocus," *Nature materials,* vol. 10, pp. 631-636, 2011.

[28] N. H. Mack, J. W. Wackerly, V. Malyarchuk, J. A. Rogers, J. S. Moore, and R. G. Nuzzo, "Optical transduction of chemical forces," *Nano letters,* vol. 7, pp. 733-737, 2007.

[29] C. Yu and J. Irudayaraj, "Multiplex biosensor using gold nanorods," *Analytical chemistry,* vol. 79, pp. 572-579, 2007.

[30] H. M. Hiep, T. Nakayama, M. Saito, S. Yamamura, Y. Takamura, and E. Tamiya, "A microfluidic chip based on localized surface plasmon resonance for real-time monitoring of antigen–antibody reactions," *Japanese Journal of Applied Physics,* vol. 47, p. 1337, 2008.

[31] S. S. Aćimović, M. A. Ortega, V. Sanz, J. Berthelot, J. L. Garcia-Cordero, J. Renger, *et al.*, "LSPR chip for parallel, rapid, and sensitive detection of cancer markers in serum," *Nano letters,* vol. 14, pp. 2636-2641, 2014.

[32] S. Lee, E. J. Cha, K. Park, S. Y. Lee, J. K. Hong, I. C. Sun, *et al.*, "A Near-Infrared-Fluorescence-Quenched Gold-Nanoparticle Imaging Probe for In Vivo Drug

Screening and Protease Activity Determination," *Angewandte Chemie,* vol. 120, pp. 2846-2849, 2008.

[33] X. Liu, M. C. Lloyd, I. V. Fedorenko, P. Bapat, T. Zhukov, and Q. Huo, "Enhanced imaging and accelerated photothermalysis of A549 human lung cancer cells by gold nanospheres," 2008.

[34] X. Huang and M. A. El-Sayed, "Gold nanoparticles: optical properties and implementations in cancer diagnosis and photothermal therapy," *Journal of Advanced Research,* vol. 1, pp. 13-28, 2010.

[35] E. Y. Hleb, J. H. Hafner, J. N. Myers, E. Y. Hanna, B. C. Rostro, S. A. Zhdanok, *et al.*, "LANTCET: elimination of solid tumor cells with photothermal bubbles generated around clusters of gold nanoparticles," 2008.

[36] S. Pillai, K. Catchpole, T. Trupke, and M. Green, "Surface plasmon enhanced silicon solar cells," *Journal of applied physics,* vol. 101, p. 093105, 2007.

[37] W. Wang, S. Wu, K. Reinhardt, Y. Lu, and S. Chen, "Broadband light absorption enhancement in thin-film silicon solar cells," *Nano letters,* vol. 10, pp. 2012-2018, 2010.

[38] H. A. Atwater and A. Polman, "Plasmonics for improved photovoltaic devices," *Nature materials,* vol. 9, pp. 205-213, 2010.

# Appendix

## Sample script language for calculating bow tie distance sweep

```
# Script file: Efficency VS wavelength.lsf

do_cross_sections = 1;

# Cross section analysis
if(do_cross_sections) {
?" Calculating scattering and absorption cross sections";

# Getting sigma cross section
sigmaabs = getsweepresult("sweep1","totalsweep");
sigmascat = getsweepresult("sweep1","scatsweep");
gap=getsweepresult("sweep1","ZR");
distance= (gap.null*1e9 +25)*2;
surface= 100*50/1e18; #calculate physical cross section of the whole bowtie
n=5; # number of legends
leg=cell(n); # define the array of strings
a=cell(n);
for (i=1:n){
leg{i}="distance="+num2str(distance(i))+" nm";

}
# Calculate cross-sections normalized to the particle area
Qscat = sigmascat.sigma/(surface); # Retrieve the parameters and attributes of datasets
Qabs = -sigmaabs.sigma/(surface);
Qext=Qscat+Qabs;
lambda = sigmaabs.lambda*1e9;
# Plot results
plot(lambda,Qabs,"lambda","Mie efficiency","Absorption cross section");
legend(leg);
plot(lambda,Qscat,"lambda","Mie efficiency","Scattering cross section");
legend(leg);
plot(lambda,Qext,"lambda","Mie efficiency","Extinction cross section");
legend(leg);
}
```